Effects of Siberian forest fires on air quality in East Asia during May 2003 and its climate implication

Jaein I. Jeong, Rokjin J. Park*, Daeok Youn

School of Earth and Environmental Science, Seoul National University, Seoul 151-742, Republic of Korea

ARTICLE INFO

ABSTRACT

In May 2003, intense forest fires occurred over Siberia, which were the largest fires in the past decade. In order to quantify the effects of these fires on regional air quality in East Asia, we used a global chemical transport model (CTM) with a biomass burning emission inventory constrained by satellite. Our focus was mainly on the enhancements of the ozone and aerosol concentrations due to these fires over East Asia. We first evaluated the model extensively by comparing the simulated and the observed ozone and aerosol concentrations at the EANET sites and found that the simulation reproduced the observed variability of those species. However, some discrepancies were found in the model when compared with the MODIS AOD observations. We tested the sensitivity of the model AOD to different injection heights of fire emissions and found that the model with an injection height of 4.5 km was in better agreement with the observations. We then used our model results to quantify the influences of Siberian forest fires on ozone and aerosols concentrations which were computed using the differences between the simulations with and without Siberian forest fire emissions. The peak increases in the surface PM_{10} and ozone concentrations were up to $90\ \mu g\,m^{-3}$ and 33 ppbv, respectively, over Siberia. In the downwind regions, the increases ranged from 5 to $30\ \mu g\,m^{-3}$ and from 3 to 20 ppbv for PM_{10} and ozone concentrations, respectively, having an important implication for air quality over East Asia. Finally, we computed the radiative forcing of aerosols and ozone from the Siberian forest fires as a measure of climate impact. Siberian forest fires were found to act mainly as a cooling agent resulting in a negative radiative forcing of $-5.8\ W\,m^{-2}$ at the surface over East Asia. The value at the TOA was $-1.5\ W\,m^{-2}$, indicating that a considerable absorption of radiation occurred in the atmosphere. This result implies that the Siberian forest fires may affect the regional climate over East Asia by intensifying atmospheric stability.

1. Introduction

Forest fires are one of the major sources of CO, volatile organic compounds (VOCs), and nitrogen oxides $NO_x \equiv NO + NO_2$ and thus have a significant effect on tropospheric ozone (Crutzen et al., 1979; DeBell et al., 2004). They also release high concentrations of aerosols into the atmosphere and result in a severe visibility degradation and harmful effects on human health (Bowman and Johnston, 2005; Park et al., 2006, 2007; In et al., 2007). The ozone precursors and aerosols from forest fires are transported over long distances, affecting air quality in downstream regions (Wotawa and Trainer, 2000; Forster et al., 2001; Wotawa et al., 2001; McKeen et al., 2002; Bertschi et al., 2004; Colarco et al., 2004; Jaffe et al., 2004; Park et al., 2007; Spracklen et al., 2007). In addition, ozone and aerosols have important climatic implications because of their

* Corresponding author. 599 Gwanak-ro, Gwanak-gu, School of Earth and Environmental Sciences, Seoul National University, Seoul 151-742, Republic of Korea. Tel.: +82 2 880 6715; fax: +82 2 883 4972.
  E-mail address: rjpark@snu.ac.kr (R.J. Park).

effects on the earth-atmosphere radiative system (Li et al., 2001; Pfister et al., 2008).

In May 2003, intense forest fires occurred in Siberia, which were recorded as one of the largest fires in Siberia in the past decade. Resulting smoke plumes and associated high aerosol optical depth (AOD) were measured by satellite (Lee et al., 2005). Surface observations also showed a significant enhancement in aerosol concentrations due to Siberian fires even in the far downwind regions (Bertschi and Jaffe, 2005; Lee et al., 2005; Nedelec et al., 2005; Lapina et al., 2006; Kaneyasu et al., 2007). The effects of those fires on air quality have been quantified in the previous studies for ozone in North America (Jaffe et al., 2004) and for column aerosols north of 75°N (Generoso et al., 2007). Because of the close proximity to the locations of the fires, East Asia must be heavily affected by the smoke plumes from these fires. However, there has been no extensive quantification of the effects of these fires on regional air quality on a daily and monthly basis in East Asia.

In this study, we use a global chemical transport model (CTM) to quantify the effects of the Siberian forest fires on regional air quality over East Asia in May 2003. Our focuses are primarily on the regional enhancements of ozone and aerosols concentrations due to the Siberian forest fires in May 2003. Although forest fires that occurred over Siberia in June 2003 were large compared with those of other years, their impacts over East Asia were much less than those in May because of 1) by a factor of two smaller emissions relative to those of May (van der Werf et al., 2006) and 2) the onset of Asian summer monsoon which accompanied large precipitation and likely scavenged the aerosols (Yihui and Chan, 2005).

The intense thermal energy which accompanies forest fires causes a rapid vertical transport of the smoke plumes into the free troposphere well above the planetary boundary layer (PBL) (Lavoué et al., 2000; Colarco et al., 2004; Fromm et al., 2005; Mazzoni et al., 2007). Recent studies have shown that smoke aerosols from forest fires reached the upper troposphere (Fromm and Servranckx, 2003; Jost et al., 2004; Turquety et al., 2007). The injection height of the forest fire emissions is one of the critical factors in determining the spatial range of fire plume transport and hence the air quality in the downwind regions. However, it has not been well constrained in the model. We also examine the sensitivity of the model to different injection heights of fire emissions by comparing the simulated results with the observations at the surface network and from the satellite measurements.

High aerosol and ozone concentrations from forest fires may perturb the radiative balance and cause a change in the regional climate (Duncan et al., 2003; Liu, 2005; Pfister et al., 2008). This issue will be of increasing importance in the future since the number of forest fires is expected to increase with increasing temperature in the warming climate (Stocks et al., 1998; Westerling et al., 2006; Soja et al., 2007; Malevsky-Malevich et al., 2008). As a measure of the climatic impact of forest fires, we use our model to estimate the radiative forcing of the aerosols and ozone from the Siberian fires, which has implications for the regional climate in East Asia.

2. Model simulations

We use the GEOS-Chem chemical transport model (version 7.04) to conduct a fully coupled oxidant-aerosol simulation (Park et al., 2006). The GEOS-Chem model uses the assimilated meteorological data from the Goddard Earth Observing System (GEOS-4) of the NASA Global Modeling and Assimilation Office (GMAO). The data include winds, convective mass fluxes, temperature, clouds, and precipitation at 6-h frequencies (3-h frequencies for surface quantities and mixing depths) with a horizontal resolution of $1° \times 1°$ and 55 hybrid pressure-sigma levels up to 0.01 hPa. We degrade these meteorological fields to a horizontal resolution of $2° \times 2.5°$ and 30 vertical levels for computational expediency.

The GEOS-Chem includes more than 80 species and 300 reactions for a detailed ozone-NO_x-hydrocarbon chemistry coupled with aerosol chemistry. Ozone simulations were evaluated extensively in the troposphere (Bey et al., 2001; Fiore et al., 2002, 2003; Hudman et al., 2004). The aerosol simulation includes H_2SO_4–HNO_3–NH_3 aerosol thermodynamics, primary organic carbon (OC) and elemental carbon (EC), secondary organic aerosol (SOA), soil dust, and sea salt (Park et al., 2003, 2004, 2005; Heald et al., 2005; Alexander et al., 2005; Fairlie et al., 2007). SOA formation follows the scheme of Chung and Seinfeld (2002). Mobilization, transport, and deposition processes of soil dust aerosols with 4 size bins were simulated using the methods described by Fairlie et al. (2007) with the Dust Entrainment and Deposition (DEAD) scheme of Zender et al. (2003a,b). The sea salt emission is computed as a function of dry particle size and local 10 m wind speed following the empirical formula from Monahan et al. (1986) (Alexander et al., 2005).

All inorganic aerosols, primary OC and EC, and SOA aerosols are considered as fine aerosols smaller than 2.5 μm in diameters and are included in $PM_{2.5}$ and PM_{10} mass concentrations in the model. Soil dust and sea salt aerosols in the model are partitioned into $PM_{2.5}$ and PM_{10} based on their sizes. For the AOD computation using aerosol dry mass concentrations, particle growth with increased relative humidity is taken into account by applying different hygroscopic growth factors to all hydrophilic species using local relative humidity conditions (Martin et al., 2003; Liu et al., 2004). We also account for the non-carbon mass attached to OC aerosol by applying a scaling factor of 2.0 to the primary OC aerosol concentration for the $PM_{2.5}$, PM_{10}, and AOD computations in the model (Turpin and Lim, 2001). We refer to the sum of OC with the non-carbon mass and SOA as organic carbon mass (OMC) hereafter.

We use the 1999–2000 global inventories of the anthropogenic emissions of NO_x, CO, VOCs, SO_x, NH_3, and primary aerosols as discussed in Park et al. (2006). The Asian emissions of NO_x, CO, VOCs, SO_x, and NH_3 defined for 60°E–158°E and 13°S–54°N are 9.1 Tg N y^{-1}, 259.8 Tg y^{-1}, 24.9 Tg C y^{-1}, 18.9 Tg S y^{-1}, and 21.8 Tg N y^{-1}, respectively. The anthropogenic emissions of primary OC and EC are from Bond et al. (2004); Asian anthropogenic OC and EC emissions are 4.9 Tg C y^{-1}, and 2.6 Tg C y^{-1}, respectively. Other emissions included those from volcanoes, lightning, the biosphere (terrestrial and marine), and biomass

burning. The details of the emissions from these sources were also as given by Park et al. (2006). Soil dust emission over Asia for May 2003 is 42.2 Tg mon^{-1}.

Biomass burning emissions for 2003 were computed using dry mass burned data with a spatial resolution of $1° \times 1°$ and monthly time resolution from the Global Fire Emissions Database (GFED) version 2 (Giglio et al., 2006; van der Werf et al., 2006), and emission factors from Andreae and Merlet (2001). The GFED inventory also provides species emissions directly but not all species are available (e.g., NH_3, SO_2, etc). Therefore, we compute biomass burning emissions as described above in the model which yields generally consistent OC emissions from fires with that of the GFED. Biomass burning emissions are distributed uniformly within the PBL in the model which is typically used as the injection height in most CTMs.

Fig. 1 shows the GFED dry mass burned data from the forest fires in Siberia (40°N–80°N, 90°E–160°E) in May for 1998–2005. The value in May 2003 is 129 Tg C by a factor of 3–10 higher than the values for other years. Table 1 compares monthly emissions of BC, OC, and CO from the Siberian forest fires during May 2003 with the climatological biomass burning inventory of Bond et al. (2004), which was previously used by Generoso et al. (2007) for the same case. Our values were higher by approximately a factor of three than the values obtained from the Bond et al. inventory. However, this discrepancy was consistent with a finding by Generoso et al. (2007), who increased the Bond et al. inventory by a similar degree in their model in order to obtain a better agreement with the observations. All simulations in this study were conducted for five months (January–May), and the first four months were used to achieve proper initialization, and we focus our attention on May when the most intense fire occurred.

3. Measurement data

We used the data from the Acid Deposition Monitoring Network (EANET, http://www.eanet.cc) and the AOD data from the Moderate Resolution Imaging Spectroradiometer (MODIS) onboard the Earth Observing System (EOS) Terra satellite and from the Aerosol Robotic Network (AERONET, http://aeronet.gsfc.nasa.gov).

EANET was initiated in April 1998 in order to improve the understanding of the acid deposition problem in East Asia. The observation sites are mainly located in islands, rural regions, and mountains in order to avoid the direct
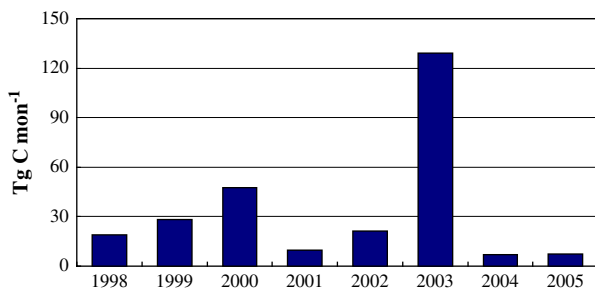
Table 1
Comparison of monthly biomass burning emissions for BC, OC, and CO in Siberia [40°N–90°N, 60°E–180°E] during May 2003.

	Bond et al. (2004)	GFED2
BC, Tg C	0.07	0.17
OC, Tg C	0.76	2.74
CO, Tg	9.86	31.26

influence of local pollution (see Fig. 2). The data have been measured on a regular basis since January 2001, including the monthly mean concentrations of gaseous pollutants (SO_2, HNO_3, NH_3, and O_3), soluble aerosols (SO_4^{2-}, NO_3^-, Cl^-, NH_4^+, Na^+, Mg^{2+}, K^+, and Ca^{2+}), and particulate matters (PM_{10}, particles less than 10 μm in aerodynamic diameter). The hourly mean concentrations of $PM_{2.5}$ (particles less than 2.5 μm in aerodynamic diameter) are also available at a couple of sites.

MODIS/Terra provides a near global coverage of AOD data at a wavelength of 550 nm measured at the local equatorial overpass time of about 10:30 am (King et al., 1999). We used the level-3 AOD products, gridded on a horizontal resolution of $1° \times 1°$ in a cloud-cleared ocean and land. MODIS-Terra AOD retrievals have the estimated uncertainty $\Delta\tau = \pm0.05 \pm 0.15\tau$ over land and $\Delta\tau = \pm0.03 \pm 0.05\tau$ over ocean (Remer et al., 2005).

AERONET measures the column-integrated AOD at visible and near-infrared wavelengths (340, 380, 440, 500, 675, 870, 940, and 1020 nm) by using a ground-based Sun photometer and derives a number of optical properties including the single scattering albedo and the Ångstrom exponent (Holben et al., 1998, 2001). We used the data from three AERONET sites (Gosan, Noto, and Shirahama) in East
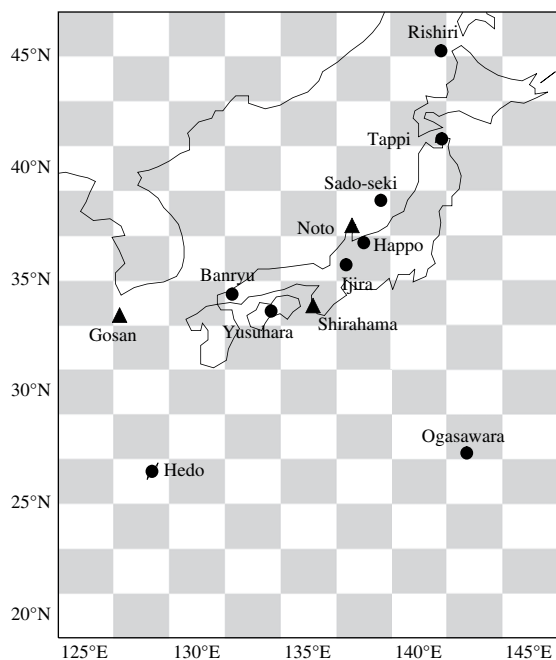

Fig. 1. Estimated dry mass burned (Tg C mon^{-1}) due to the Siberian forest fires in May for 1998–2005 from the GFED inventory.

Fig. 2. Sites from the Acid Deposition Monitoring Network in East Asia (EANET; closed circles) and Aerosol Robotic Network (AERONET; closed triangles) in 2003. Boxes indicate the $2° \times 2.5°$ model grids.

Asia (see Fig. 2). The AOD values at 550 nm (the approximate midpoint of the 440-nm and 675-nm AERONET channels) were obtained by interpolating the values at 440 nm and 675 nm because the data at 500 nm were not available for the Gosan and Noto sites (Chung et al., 2005).

4. Model evaluation

Fig. 3 shows the time series of the simulated and observed hourly mean $PM_{2.5}$ mass concentrations at the Rishiri site (45.1°N, 141.2°E). A peak value of up to 108 $\mu g \, m^{-3}$ was observed on May 7. The values for May 4–7 and on May 14 were by a factor of 3–5 higher than the monthly mean concentration of 23 $\mu g \, m^{-3}$ and reflect significant fire influences on $PM_{2.5}$ concentrations. The model generally captured the temporal variation of the observed $PM_{2.5}$ concentrations.

Fig. 3 also shows the time series of the simulated and observed daily mean AOD values at the three AERONET sites: Gosan, Noto, and Shirahama. The observed values in early May were generally lower than 0.5, reflecting the fact that those sites are located in relatively clean areas. However, they increased up to 1.2 during May 16–25 due to the Siberian forest fires. Observations in Gwangju, South Korea, during the same period also showed a similar increase in the daily mean AOD of up to 1.5 (Lee et al., 2005). The simulated AOD values in early May are by a factor of 2 higher than the observations especially at Gosan and Noto sites because of too high sulfate aerosol concentrations in the model (not shown). Whereas, OC aerosol from the Siberian forest fires is the main contributor to the simulated AOD during May 18–25. The model

generally reproduced increases in AODs at the AERONET sites in May 16–25 except for the Shirahama site (shaded in Fig. 3b).

It is noted that the influence of the fires on the AOD values at the AERONET sites was shown later relative to those on the $PM_{2.5}$ concentrations at Rishiri. This difference in the timings of fire influences at different observation locations is examined using the back trajectories analysis by the HYSPLIT model (http://www.arl.noaa.gov/ready/open/hysplit4.html) (not shown). Results indicated that fire plumes were transported eastward in early May but southward later (Murayama et al., 2004; Lee et al., 2005; Kaneyasu et al., 2007). As shown in Fig. 3 the model also captured this different peak timing of $PM_{2.5}$ and AOD at different sites.

Fig. 4 shows the spatial distributions of monthly mean AOD values at 550 nm from the model and the MODIS observations. The model results were sampled at 0900–1200 local time for the days and locations in which the MODIS observations were available. The observed AODs are high in eastern China and in northwestern Pacific Ocean, reflecting high anthropogenic emissions and their transport to the Pacific (Heald et al., 2006). The simulated AODs also show a similar spatial pattern but are lower than the observations especially over the northwestern Pacific. We will further examine this discrepancy in AOD between the model and the MODIS observations below.

Fig. 5 presents scatter-plot comparisons of the simulated versus observed monthly means of PM_{10} and ozone concentrations in surface air and AOD values in May for the ensemble of the three-year data (2002–2004) at the EANET sites. Our main focus is on May 2003 but due to the limited
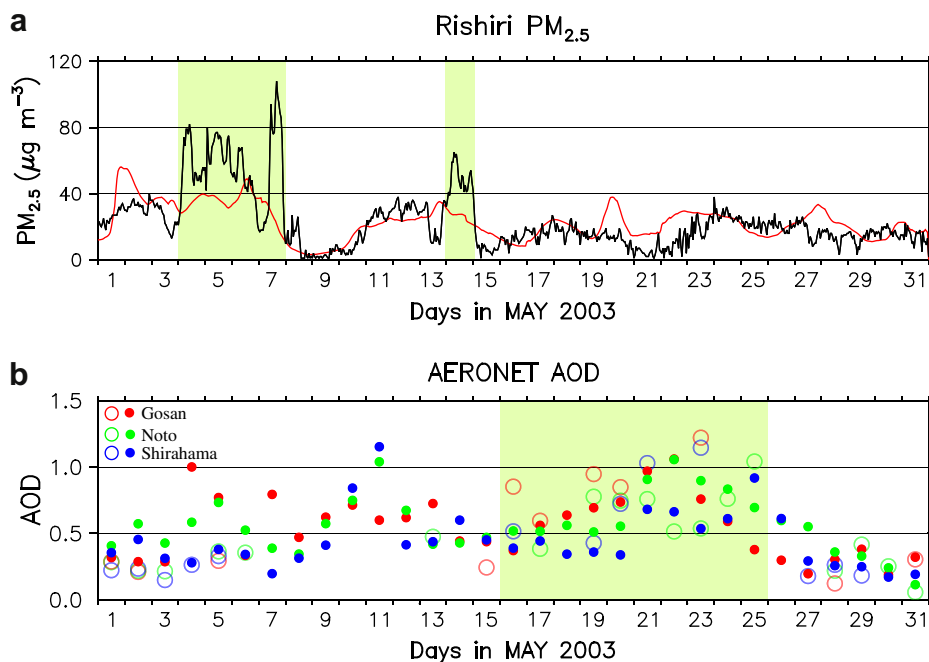

Fig. 3. Time series data of (a) simulated (red line) and observed (black line) hourly $PM_{2.5}$ concentrations at the Rishiri site of the EANET, and (b) simulated (closed circle) and observed (open circle) daily AOD values at Gosan (red), Noto (green), and Shirahama (blue) AERONET sites (For interpretation of the references to color in this figure, the reader is referred to the web version of this article).
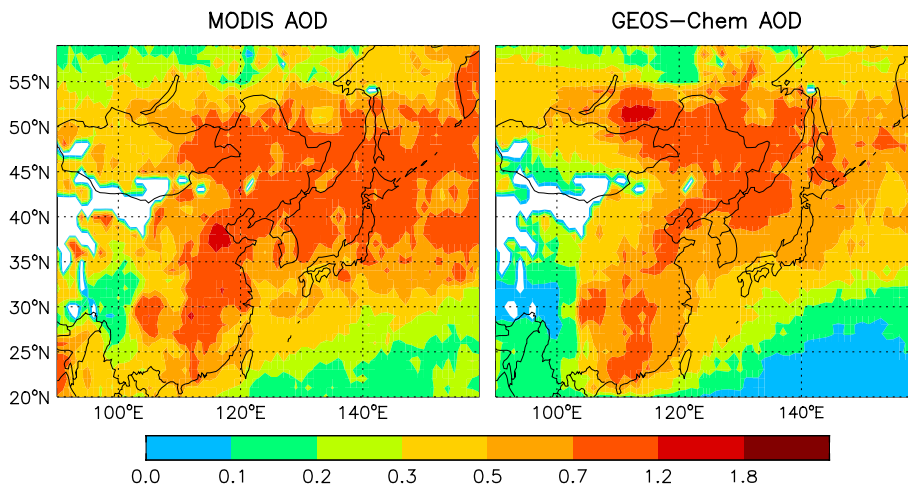
Fig. 4. Monthly mean AOD at 550 nm from the MODIS (left) and the model (right) for May 2003. White areas indicate missing data (For interpretation of the references to color in this figure, the reader is referred to the web version of this article).

number of observations at the EANET sites we extend our evaluation including the values in May for three consecutive years (2002–2004).

For PM_{10} concentrations in surface air, R^2 between the model and the observation is 0.33 and regression slope is 0.93. However, the AOD comparison shows a 50% low bias in the model relative to the MODIS observations for May 2002–2004 despite a relatively high R^2 value (0.68). Significant underestimates in the model were mostly found at the northern EANET sites in 2003 (closed circles). These discrepancies may be due to errors associated with the forest fire simulations in the model, which will be discussed in Section 5.

Fig. 6 shows site-by-site comparisons of the simulated and the observed monthly mean PM_{10} concentrations at the EANET sites in May 2003. The simulated values were also broken down by the type of species in different colors (bars). The observed values were higher in the north than in the south. The model also shows a similar pattern. We found that the largest contributions to the simulated PM_{10} concentrations were from soil dust and OMC aerosols. The high concentrations of soil dust aerosols were mainly from the arid regions in China and Mongolia (30°N–50°N,

80°E–110°E) where dust storms typically occur in spring (Zhang et al., 1993; Husar et al., 2001; Park and In, 2003). The previous study by Fairlie et al. (2007) has shown that the GEOS-Chem model captured the amplitude and seasonal cycle in dust aerosols at surface sites in the Northern Pacific. OMC aerosol concentrations were especially high at the northern sites (>35°N), and these aerosols were mainly primary OC from the Siberian forest fires. A quantification of the influences of these fires on the PM_{10} concentrations over East Asia will be discussed in Section 6.

A comparison of the monthly mean AOD values between the model and the MODIS observation sampled at the EANET sites are also shown in Fig. 6. Relative to the PM_{10} comparisons discussed above, we found large discrepancies between the simulated and observed AOD values. In particular, at the northern sites such as Rishiri, Tappi, and Sado-seki, the model was by a factor of two lower than the MODIS observations. These northern sites were significantly affected by Siberian forest fires particularly in early May (Fig. 3). There was also a good agreement between the model and the MODIS observation at the southern EANET sites (Yusuhara, Hedo, and Ogasawara) where the influences of the Siberian forest fires were
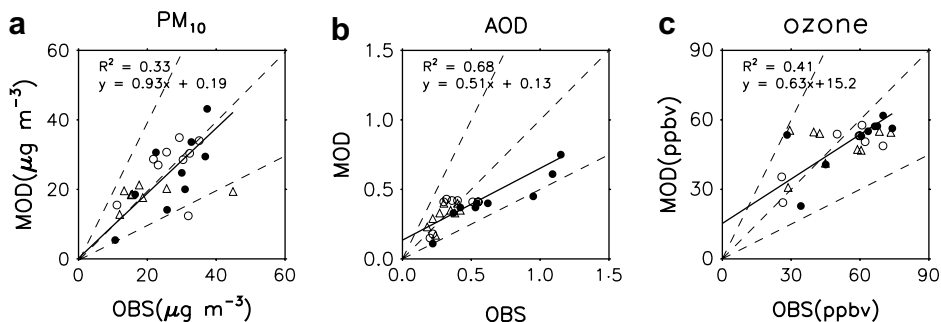

Fig. 5. Scatter plots of the observed and the simulated monthly mean (a) PM_{10} and (c) daytime ozone concentrations (averaged for 1300–1700 local time) and (b) AOD at 550 nm at EANET sites in May 2002 (triangles), May 2003 (closed circles) and May 2004 (open circles). Reduced major axis regressions for the ensemble of the data (thin line) are shown; R^2 and regression equations are shown inset. Dashed lines denote a factor of 2 departure.
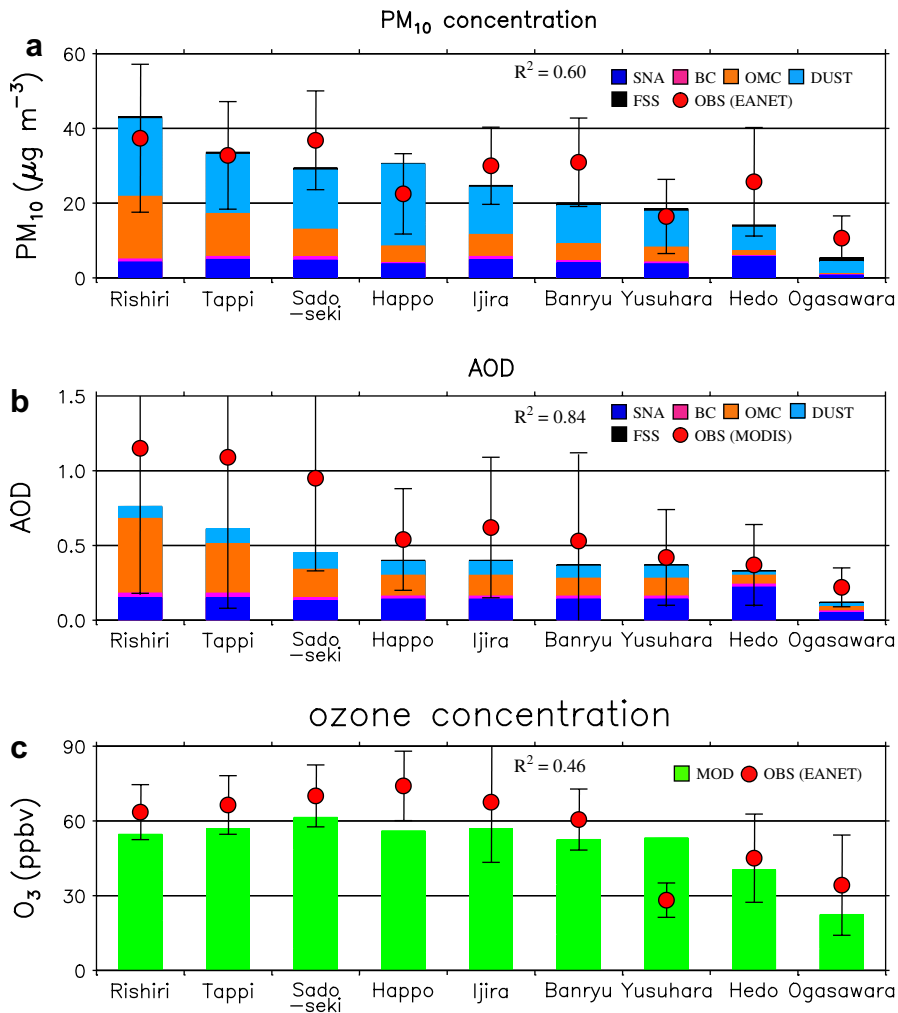
Fig. 6. Comparisons of the observed (red circles) and the simulated (large bars) monthly mean values for (a) PM$_{10}$ and (c) daytime ozone concentrations, and (b) AOD at 550 nm sampled at EANET sites in May 2003. The PM$_{10}$ and ozone concentrations are in surface air from the EANET and the AOD observations are from the MODIS. Vertical error bars represent one standard deviation with respect to the observed daily mean concentrations, respectively. Simulated contributions of secondary inorganic aerosol (SNA), black carbon (BC), organic carbon mass (OMC), soil dust (DUST), and fine mode sea-salt (FSS) aerosols to PM$_{10}$ concentrations and AOD values are denoted in different colors. OMC aerosols include primary OC with non-carbon mass and SOA (For interpretation of the references to color in this figure, the reader is referred to the web version of this article).

important later in May, and their contributions were relatively smaller. The low biases in the simulated AOD at the northern sites may be caused by errors in the simulation of Siberian fire emissions by the model. We have examined this issue in Section 5 by performing several sensitivity runs with different injection heights and magnitudes of emissions.

For the evaluation of ozone in the model, we used the monthly means computed by using the hourly ozone concentrations during the daytime (1300–1700 local time) with a deep mixed layer. The nighttime surface ozone simulated by the model was inadequate for a comparison with the observations because the vertical resolution of this model in the boundary layer was too coarse to accurately simulate the nighttime shallow mixing depth (Fiore et al., 2002). The model explained about 40% of the observed variability for the ensemble of 2002–2004 observations

(panel c in Fig. 5). However, the simulated concentrations were lower by 40% relative to the observations, and the biggest discrepancies occurred at the Yusuhara site (33.4°N, 132.9°E) where values were 29 and 28 ppbv for 2002 and 2003, respectively (triangle and closed circle in the upper left). Yusuhara site is located in mountain with its elevation of 225 m. When compared to the values at the nearby Banryu site (60 m elevation) which is in the same model grid they are still very low. Too coarse model spatial resolution could be a possible reason for this but still there is no clear reason for the model bias at the Yusuhara site.

Fig. 6 also compares the simulated and the observed monthly mean ozone concentrations at individual EANET sites in May 2003. The simulated values were generally lower than the observations but were within one standard deviation except for Happo and Yusuhara. The model reproduced the spatial variability in observations

reasonably well ($R^2 = 0.46$) with a 30% low bias (regression slope $= 0.72$), which was similar to the evaluation with the three years (2002–2004). The largest discrepancy occurred at the Yusuhara site where the model was by a factor of two higher than the observation. Excluding the Yusuhara site from the analysis would increase the value of R^2 to 0.9, indicating a successful ozone simulation by the model.

5. Sensitivity simulations with different injection heights

In this section we tested the sensitivity of the model to different injection heights in order to examine possible reasons for the discrepancies in the simulated AOD values discussed in Section 4. Two sensitivity simulations with the injection heights of 3 and 4.5 km were conducted. These heights were chosen on the basis of the lidar observations of smoke aerosols in the downwind regions during May 2003 (Mattis et al., 2003; Murayama et al., 2004).

Fig. 7 summarizes the simulated monthly mean PM_{10} and ozone concentrations in surface air and AOD values at the EANET sites from the models with the injection heights of 3 km (CASE1) and 4.5 km (CASE2), respectively, together with the observations. A higher injection height tends to decrease PM_{10} concentrations at three northern sites (Rishiri, Tappi, and Sado-seki) but to increase them at other sites further south, indicating more efficient long-range transport as smoke plumes were lifted upward. The largest increase was found at Happo because of its high elevation (1850 m).

The impact of the different injection heights on the simulated monthly mean AOD is also shown in Fig. 7. As the injection height increases, the simulated AOD also increases and is in better agreement with the MODIS AOD at the EANET sites. This is probably because aerosols released into the free troposphere are less influenced by scavenging processes. In addition, aerosols in the free troposphere are efficiently transported with faster winds and thus affect the downwind regions. Although the use of
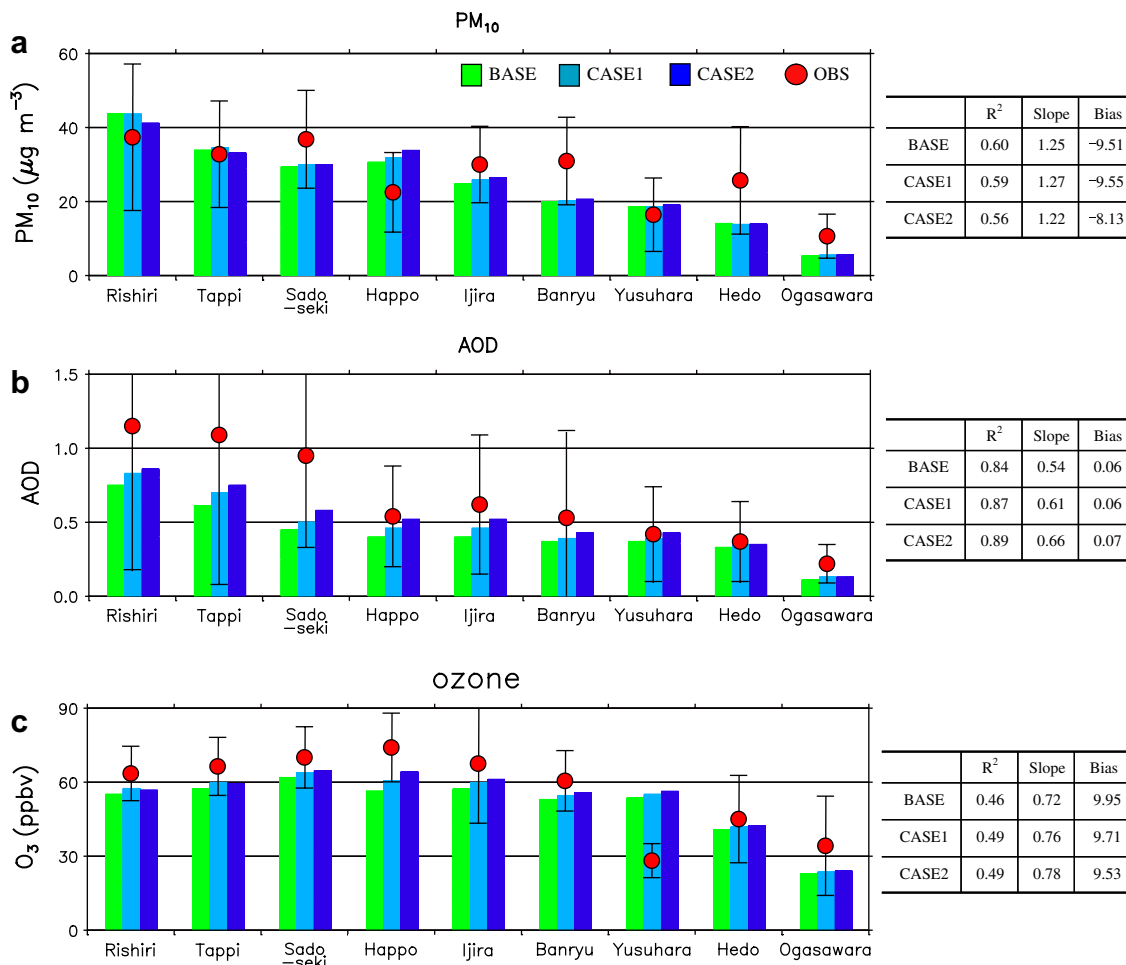

Fig. 7. Same as in Fig. 6 but with two more sensitivity model results using 3.0 km (CASE1) and 4.5 km (CASE2) injection heights of the Siberian fire emissions. Red circles indicate the observations with the standard deviation (vertical error bars). Green, skyblue, and blue bars indicate the standard, CASE1, and CASE2 sensitivity simulations, respectively. Statistics including the coefficient of determination (R^2), reduced major axis regression (Slope), and mean bias (Bias) are shown in the right panel (For interpretation of the references to color in this figure, the reader is referred to the web version of this article).

higher injection heights improve the simulated AOD values relative to the MODIS observations, large discrepancies still remain at the three northern sites.

Simulated ozone concentrations with different injection heights showed responses similar to the ones for the PM_{10} concentrations. The bias and R^2 values exhibited minimal changes from the standard simulation, reflecting a dominant contribution of the anthropogenic sources to the ozone precursor emissions in East Asia.

We also conducted an additional sensitivity simulation with an injection height of 4.5 km and with doubled fire emissions in May 2003 (not shown) to examine errors with the magnitude of biomass burning emissions in the model. The resulting monthly mean AOD increases by a factor of two relative to that of the standard simulation and is in much closer agreement with the MODIS AOD (regression slope increased from 0.54 to 1.21). However, the monthly mean surface PM_{10} concentrations at the EANET sites are too high compared with the observations (regression slope = 1.68). We could not find any conclusive results from these experiments to explain the model biases.

The similar low biases in the model compared with the MODIS AOD observations over the North Pacific as shown in Fig. 4 were also found in previous studies (Heald et al., 2006; Generoso et al., 2007). MODIS AOD observations were generally reported to be higher than the ground-based measurements (Chin et al., 2004; Matsui et al., 2004; Chu et al., 2005; Remer et al., 2005; Schaapa et al., 2008).

Moreover, different optical properties and assumptions used for the model and for the MODIS retrieval algorithm could contribute to different AOD values between the two. The MODIS AOD algorithm determines three aerosol types (soluble, dust, and soot) over land, and fine mode (water soluble and water soluble with humidity) and coarse mode (sea salt and dust) over ocean (Remer et al., 2005). The GEOS-Chem carries a larger number of aerosols species and computes AOD for each with different refractive indices but mixing between species is not accounted for. The spherical assumption even for the nonspherical dust aerosols in the model could contribute to the bias as well. As shown in Heald et al. (2005) simulated SOA is still too low relative to the observations in the northwestern Pacific which could contribute to the discrepancy in the simulated AOD. This issue certainly needs further investigation in the future.
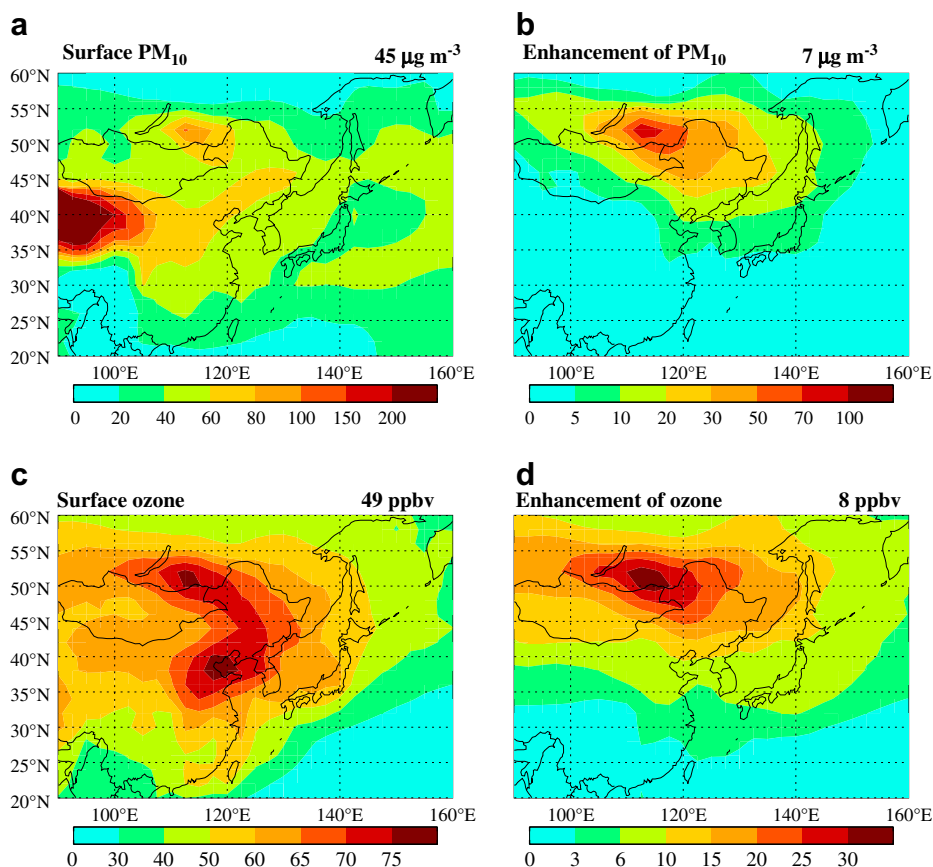

Fig. 8. Spatial distributions of the simulated monthly mean (a) PM_{10} and (c) daytime ozone concentrations at the surface from our best simulation with 4.5 km injection height (CASE2 simulation in Section 5). The enhancements in (b) PM_{10} and (d) daytime ozone concentrations due to the Siberian forest fires were computed by subtracting the simulation without the fire emissions from the CASE2 simulation. The domain-averaged values are shown in the upper right corner of each panel.

6. Influences of Siberian forest fires on surface PM$_{10}$ and ozone concentrations

We use our best simulation (CASE2 with an injection height of 4.5 km) in Section 5 to quantify the effects of the Siberian forest fires on PM$_{10}$ and ozone concentrations over East Asia in May 2003. Differences between simulations with and without fire emissions are used to determine enhancements in concentrations due to the fires.

Fig. 8 shows the spatial distributions of the simulated monthly mean PM$_{10}$ and daytime ozone concentrations in surface air over East Asia in May 2003. The enhancements in the PM$_{10}$ and ozone concentrations due to the Siberian fires are also shown in the figure. The simulated monthly mean PM$_{10}$ concentrations were the highest in western China and Siberia. The high values over western China were mainly due to the soil dust aerosol from the desert, whereas those over Siberia were predominantly OC aerosol from the forest fires, accounting for 75–90% of fire aerosols in the model. The highest increase in PM$_{10}$ concentration is up to 90 µg m^{-3} over Siberia on a monthly mean basis. The increases in the downwind regions ranged from 5 to 30 µg m^{-3} (the domain average of 7 µg m^{-3}), which significantly amount to the annual average PM$_{10}$ standard

(50 µg m^{-3}) in Korea (KME, 2007). The relative contributions of the fire aerosols to the monthly mean total PM$_{10}$ concentration were more than 80% in Siberia and 15–30% over Korea and Japan, having an important implication for the regulation of air quality with respect to the PM concentrations.

The simulated monthly mean ozone concentrations show a slightly different spatial distribution such that high ozone concentrations are in eastern China and Siberia (Fig. 8c). The high ozone concentrations in eastern China reflect the primary source region of anthropogenic emissions. The enhancements in the monthly mean surface ozone concentrations (Fig. 8d) show a similar spatial pattern to that of the PM$_{10}$ concentrations. Resulting increases in ozone concentrations are up to 33 ppbv in Siberia and range from 3 to 20 ppbv in the downwind regions. These ozone increases account for 5–33% of the 8-h average ozone standard (60 ppbv) in Korea (Jo and Park, 2005), implying that the ozone air quality can also be significantly affected by forest fires over East Asia.

As smoke plumes are transported away from the fires, they are mixed with surrounding air by turbulence and the effects of forest fires gradually decrease. Real et al. (2007) used observed CO and ozone concentrations to show the
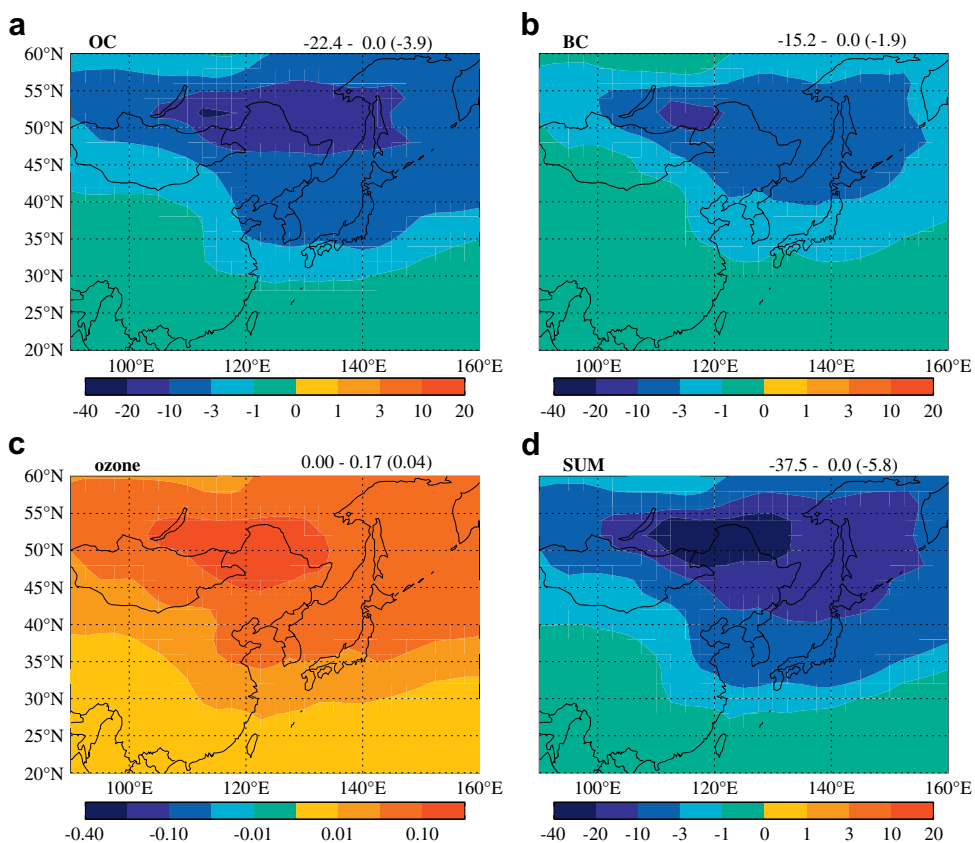

Fig. 9. Monthly mean surface radiative forcing (W m^{-2}) of (a) OC, (b) BC, and (c) ozone from the Siberian forest fires over East Asia. Surface radiative forcing is computed as differences in net downward fluxes at the surface between the models with and without the Siberian forest fires emissions. The bottom right panel shows the sum of those three. The domain minimum and maximum values are given on the upper right corner of each panel; numbers in parentheses represent the mean values of the domains.

mixing and dilution of fire plumes with surrounding air. Their approach is sensitive to the background concentrations of those species. Here we use the simulated enhancements of the PM_{10} and ozone concentrations due to the Siberian fires to compute dilution factors, reflecting the mixing and dilution of fire plumes as they are transported. The dilution factor is defined as the ratio of enhancements in ozone and aerosol concentrations over the fire locations to those over the downwind regions. Our simulated enhancements of the monthly mean PM_{10} concentrations in surface air due to the Siberian forest fires decreased from 90 μg m^{-3} over the fires to 7 μg m^{-3} in East Asia, yielding a dilution factor of 13. Whereas, ozone dilution factor is 4 (decreased from 33 ppbv to 8 ppbv) and is by a factor of 3 smaller than that of aerosol presumably because of continued ozone formation in transit despite the photochemical reduction due to the fire aerosols (Real et al., 2007). This may indicate that forest fires could be more important for ozone concentrations in the context of long-range transport of pollution.

7. Radiative impacts

Fire aerosol and ozone concentrations discussed in Section 6 not only have a significant implication for air quality in East Asia but are also important with respect to climate because of their scattering and absorption of solar and terrestrial radiations. We applied our best estimates to compute the radiative forcing of ozone and aerosols from the Siberian forest fires over East Asia as a measure of the climate impact.

We use the National Center for Atmospheric Research (NCAR) Column Radiation Model (CRM; Briegleb, 1992; Kiehl et al., 1998) for radiative transfer calculation with a δ-Eddington approximation using 18 spectral intervals. Optical properties of individual aerosols such as aerosol optical depth (τ), single scattering albedo (ω), asymmetry factor (g) and forward scattering factor were precomputed using a Mie algorithm (Wiscombe, 1980) and provided to the NCAR-CRM. The simulated ozone concentrations are directly used as input for the NCAR-CRM computation. Radiative forcing of fire aerosols and ozone is defined as differences in net downward fluxes between results with and without fire aerosols and ozone. Fire aerosols were mostly composed of OC and BC aerosols as discussed in Section 6.

Fig. 9 shows the radiative forcing of OC, BC, and ozone at the surface due to the Siberian fires in May 2003. The extrema and averaged values for the domain in W m^{-2} are denoted in the upper right corner of each panel in the figure. Fire OC and BC aerosols result in negative forcing of -3.9 and -1.9 W m^{-2} averaged over the whole domain
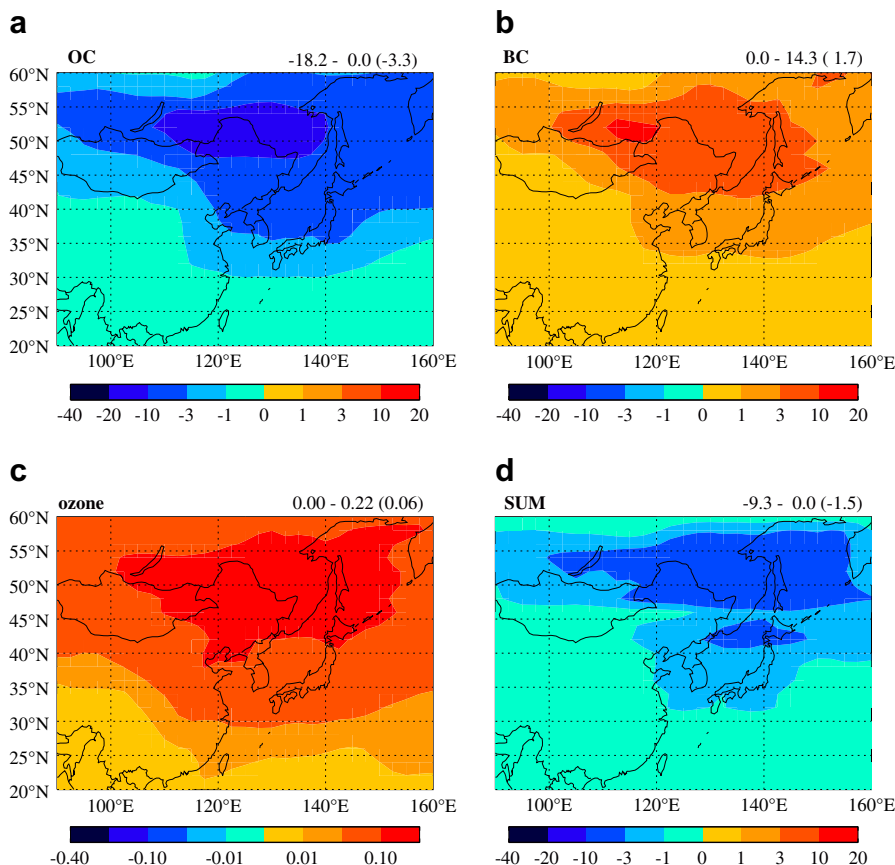

Fig. 10. Same as in Fig. 9 but at the TOA.

at the surface in East Asia. Peak OC and BC radiative forcing of up to -22 and $-15\,W\,m^{-2}$ are found over the fire locations. Despite a smaller fraction of BC aerosol concentrations among fire aerosols (less than 10%), the resulting negative forcing at the surface is significant. On the other hand, ozone shows a small positive radiative forcing at the surface. The total radiative forcing, sum of OC, BC, and ozone radiative forcing, peaks up to $-37.5\,W\,m^{-2}$. The total domain-averaged radiative forcing is $-5.8\,W\,m^{-2}$, indicating the climatic cooling effect of Siberian fires at the surface.

The radiative forcing at the top of the atmosphere (TOA) is presented in Fig. 10. The spatial distributions and magnitudes of TOA forcing are similar to those at the surface (Fig. 9) except for BC aerosol. The BC radiative forcing averaged over the whole domain is $1.7\,W\,m^{-2}$ at the TOA. This positive TOA BC forcing implies that substantial solar absorption occurs in the atmosphere. The total radiative forcing at the TOA averaged over the whole domain is $-1.5\,W\,m^{-2}$ smaller than that of the surface, indicating that $4.3\,W\,m^{-2}$ is absorbed mostly by the BC in the atmosphere. Our mean forcing at the TOA was found to be comparable with that obtained in an earlier study by Pfister et al. (2008) who calculated the OC, BC, and ozone radiative forcing and their sum, $-4.4 \pm 2.4\,W\,m^{-2}$, from the summer 2004 Alaska fires.

8. Conclusions

In May 2003, intense forest fires occurred in Siberia, the largest fire in the past decade. In this study, we have quantified the effects of the Siberia forest fires on regional enhancements of ozone and aerosols concentrations and their impact on the radiative forcing over East Asia using a 3-D global chemical transport model (GEOS-Chem).

First, we extensively evaluated our model by comparing the simulated and observed ozone and aerosol concentrations at the EANET sites and AOD values from the MODIS satellite. The results showed a generally successful simulation of capturing the observed spatial variability with the high R^2 values for PM_{10} ($R^2 = 0.60$) and ozone ($R^2 = 0.91$, excluding Yusuhara) at the EANET sites. The R^2 between the model and the MODIS AOD sampled at the EANET sites was also high ($R^2 = 0.84$) but there were low biases in the model, especially at the northern EANET sites.

We examined the sensitivity of the model to the vertical extent of fire emissions using different injection heights. As the injection height increased, the simulated monthly mean surface PM_{10} concentrations and AOD were in better agreement with the surface and the satellite observations over East Asia. However, the use of higher injection height in the model did not fully resolve the discrepancy in AOD between the model and the MODIS observations.

We also quantified the enhancements of the monthly mean PM_{10} and daytime ozone concentrations due to the Siberian forest fires by using our best simulations. The peak increases in surface PM_{10} and ozone concentrations were up to $90\,\mu g\,m^{-3}$ and 33 ppbv, respectively. Fire influences were extended to the far downwind areas where the increases in PM_{10} and ozone concentrations ranged from 5

to $30\,\mu g\,m^{-3}$ and from 3 to 20 ppbv, respectively. They accounted for 10–60% and 5–33% of the annual average PM_{10} and 8-h average ozone standards in Korea, respectively, having a significant implication for air quality over East Asia.

The radiative forcing of ozone and aerosols from Siberian forest fires was computed as a measure of climatic impact over East Asia. We found that Siberian forest fires predominantly acted as a cooling agent resulting in a negative radiative forcing of $-5.8\,W\,m^{-2}$ at the surface over East Asia. The peak value was $-37.5\,W\,m^{-2}$ over Siberia. The value at the TOA was $-1.5\,W\,m^{-2}$ over East Asia, indicating that a considerable absorption of radiation occurred in the atmosphere. The BC aerosol from fires was the main contributor to the absorption of solar radiation, causing atmospheric heating. This result implied that forest fires may affect the regional climate by intensifying the atmospheric stability and thus affect the regional climate by changing the meteorological fields. An accurate quantification of the influences of the Siberian fires on air quality and climate over East Asia has a growing importance since fires in Siberia are expected to occur more frequently in the future warming climate.

Although we quantified the effects of the May 2003 Siberian fires on air quality and climate over East Asia using our best simulation, some limitation of our work must be acknowledged. Our model simulations did not fully account for the temporal variability of fire emissions which may cause differences in their effects on the downwind regions. There are also large unresolved discrepancies in AODs between the model and the MODIS observations over East Asia. Several uncertainties in the model, including underestimates of SOA in the free troposphere, the spherical assumption for all soil dust aerosols, and different optical properties used for the AOD computations may be possible contributors. Further work is necessary to examine those uncertainties in the model to resolve the discrepancies in AOD values between the model and the MODIS observations over East Asia.

References

Alexander, B., Park, R.J., Jacob, D.J., Li, Q.B., Yantosca, R.M., Savarino, J., Lee, C.C.W., Thiemens, M.H., 2005. Sulfate formation in sea-salt aerosols: constraints from oxygen isotopes. Journal of Geophysical Research 110, D10307. doi:10.1029/2004JD005659.

Andreae, M.O., Merlet, P., 2001. Emission of trace gases and aerosols from biomass burning. Global Biogeochemical Cycles 15, 955–966.

Bertschi, I.T., Jaffe, D.A., 2005. Long-range transport of ozone, carbon monoxide, and aerosols to the NE Pacific troposphere during the summer of 2003: observations of smoke plumes from Asian boreal fires. Journal of Geophysical Research 110, D05303. doi:10.1029/2004JD005135.

Bertschi, I.T., Jaffe, D.A., Jaeglé, L., Price, H.U., Dennison, J.B., 2004. PHO-BEA/ITCT 2002 airborne observations of transpacific transport of ozone, CO, volatile organic compounds, and aerosols to the northeast Pacific: impacts of Asian anthropogenic and Siberian boreal fire

emissions. Journal of Geophysical Research 109, D23S12. doi:10.1029/2003JD004328.

Bey, I., Jacob, D.J., Yantosca, R.M., Logan, J.A., Field, B., Fiore, A.M., Li, Q., Liu, H., Mickley, L.J., Schultz, M., 2001. Global modeling of tropospheric chemistry with assimilated meteorology: model description and evaluation. Journal of Geophysical Research 106, 23,073–23,096.

Bond, T.C., Streets, D.G., Yarber, K.F., Nelson, S.M., Woo, J.-H., Klimont, Z., 2004. A technology-based global inventory of black and organic carbon emissions from combustion. Journal of Geophysical Research 109, D14203. doi:10.1029/2003JD003697.

Bowman, D.M.J.S., Johnston, F.H., 2005. Wildfire smoke, fire management, and human health. EcoHealth 2 (1), 76–80.

Brieglib, B.P., 1992. Delta-Eddington approximation for solar radiation in the NCAR community Climate Model. Journal of Geophysical Research 97, 7603–7612.

Chin, M., Chu, A., Levy, R., Remer, L., Kaufman, Y., Holben, B., Eck, T., Ginoux, P., Gao, Q., 2004. Aerosol distribution in the Northern Hemisphere during ACE-Asia: results from global model, satellite observations, and Sun photometer measurements. Journal of Geophysical Research 109, D23S90. doi:10.1029/2004JD004829.

Chu, D.A., Remer, L.A., Kaufman, Y.J., Schmid, B., Redemann, J., Knobelspiesse, K., Chern, J.-D., Livingston, J., Russell, P.B., Xiong, X., Ridgway, W., 2005. Evaluation of aerosol properties over ocean from moderate resolution imaging spectroradiometer (MODIS) during ACE-Asia. Journal of Geophysical Research 110, D07308.

Chung, C.E., Ramanathan, V., Kim, D., Podgorny, I.A., 2005. Global anthropogenic aerosol direct forcing derived from satellite and ground-based observations. Journal of Geophysical Research 110, D07308. doi:10.1029/2005JD006356.

Chung, S.H., Seinfeld, J.H., 2002. Global distribution and climate forcing of carbonaceous aerosols. Journal of Geophysical Research 107 (D19), 4407. doi:10.1029/2001JD001397.

Colarco, P.R., Schoeberl, M.R., Doddridge, B.G., Marufu, L.T., Torres, O., Welton, E.J., 2004. Transport of smoke from Canadian forest fires to the surface near Washington, D.C.: injection height, entrainment, and optical properties. Journal of Geophysical Research 109, D06203. doi:10.1029/2003JD004248.

Crutzen, P.J., Heidt, L.E., Krasnec, P.K., Pollack, W.H., Seiler, W., 1979. Biomass burning as a source of atmospheric CO, H_2, N_2O, NO, CH_3Cl, and COS. Nature 282, 253–279.

DeBell, L.J., Talbot, R.W., Dibb, J.E., Munger, J.W., Fischer, E.V., Frolking, S.E., 2004. A major regional air pollution event in the northeastern United States caused by extensive forest fires in Quebec, Canada. Journal of Geophysical Research 109, D19305. doi:10.1029/2004JD004840.

Duncan, B.N., Bey, I., Chin, M., Mickley, L.J., Fairlie, T.D., Martin, R.V., Matsueda, H., 2003. Indonesian wildfires of 1997: impact on tropospheric chemistry. Journal of Geophysical Research 108 (D15), 4458. doi:10.1029/2002JD003195.

Fairlie, T.D., Jacob, D.J., Park, R.J., 2007. The impact of transpacific transport of mineral dust in the United States. Atmospheric Environment 41, 1251–1266.

Fiore, A.M., Jacob, D.J., Bey, I., Yantosca, R.M., Field, B.D., Fusco, A.C., Wilkinson, J.G., 2002. Background ozone over the United States in summer: origin, trend, and contribution to pollution episodes. Journal of Geophysical Research 107 (D15). doi:10.1029/2001JD000982.

Fiore, A.M., Jacob, D.J., Mathur, R., Martin, R.V., 2003. Application of empirical orthogonal functions to evaluate ozone simulations for the eastern United States with regional and global models. Journal of Geophysical Research 108, 4431. doi:10.1029/2002JD003151.

Forster, C., Wandinger, U., Wotawa, G., James, P., Mattis, I., Althausen, D., Simmonds, P., O'Doherty, S., Jennings, S.G., Kleefeld, C., Schneider, J., Trickl, T., Kreipl, S., Jager, H., Stohl, A., 2001. Transport of boreal forest fire emissions from Canada to Europe. Journal of Geophysical Research 106 (D19), 22,887–22,906.

Fromm, M., Bevilacqua, R., Servranckx, R., Rosen, J., Thayer, J.P., Herman, J., Larko, D., 2005. Pyro-cumulonimbus injection of smoke to the stratosphere: observations and impact of a super blowup in northwestern Canada on 3–4 August 1998. Journal of Geophysical Research 110, D08205. doi:10.1029/2004JD005350.

Fromm, M.D., Servranckx, R., 2003. Transport of forest fire smoke above the tropopause by supercell convection. Geophysical Research Letters 30 (11), 1542. doi:10.1029/2002GL016820.

Generoso, S., Bey, I., Attié, J.-L., Bréon, F.-M., 2007. A satellite- and model-based assessment of the 2003 Russian fires: impact on the Arctic region. Journal of Geophysical Research 112, D15302. doi:10.1029/2006JD008344.

Giglio, L., van der Werf, G.R., Randerson, J.T., Collatz, G.J., Kasibhatla, P.S., 2006. Global estimation of burned area using MODIS active fire observations. Atmospheric Chemistry and Physics 6, 11091–11141.

Heald, C.L., Jacob, D.J., Park, R.J., Alexander, B., Fairlie, T.D., Yantosca, R.M., Chu, D.A., 2006. Transpacific transport of Asian anthropogenic aerosols and its impact on surface air quality in the United States. Journal of Geophysical Research 111, D14310. doi:10.1029/2005JD006847.

Heald, C.L., Jacob, D.J., Park, R.J., Russell, L.M., Huebert, B.J., Seinfeld, J.H., Liao, H., Weber, R., 2005. A large organic aerosol source in the free troposphere missing from current models. Geophysical Research Letters 32, L18809. doi:10.1029/2005GL023831.

Holben, B.N., Eck, T.F., Slutsker, I., Tanre, D., Buis, J.P., Setzer, A., Vermote, E., Reagan, J.A., Kaufman, Y.J., Nakajima, T., Lavenu, F., Jankowiak, I., Smirnov, A., 1998. AERONET: a federated instrument network and data archive for aerosol characterization. Remote Sensing of Environment 66, 1–16.

Holben, B.N., Tanre, D., Smirnov, A., Eck, T.F., Slutsker, I., Abuhassa, N., Newcomb, W.W., Schafer, J.S., Chatenet, B., Lavernu, F., Kaufman, Y.J., Vande Castle, J., Setzer, A., Markham, B., Clark, D., Rouin, R., Halthore, R., Karneli, A., O'Neil, N.T., Piertras, C., Pinker, R.T., Voss, K., Zibordi, G., 2001. An emerging ground-based aerosol climatology: aerosol optical depth from AERONET. Journal of Geophysical Research 106, 12067–12097.

Hudman, R.C., Jacob, D.J., Cooper, O.C., Evans, M.J., Heald, C.L., Park, R.J., Fehsenfeld, F., Flocke, F., Holloway, J., Hubler, G., Kita, K., Koike, M., Kondo, Y., Neuman, A., Nowak, J., Oltmans, S., Parrish, D., Roberts, J.M., Ryerson, T., 2004. Ozone production in transpacific Asian pollution plumes and implications for ozone air quality in California. Journal of Geophysical Research 109, D23S10. doi:10.1029/2004JD004974.

Husar, R.B., Tratt, D.M., Schichtel, B.A., Falke, S.R., Li, F., Jaffe, D., Gasso, S., Gill, T., Laulainen, N.S., Lu, F., Reheis, M.C., Chun, Y., Westphal, D., Holben, B.N., Guymard, C., McKendry, I., Kuring, N., Feldman, G.C., McClain, C., Frouin, R., Merrill, J., DuBois, D., Vignola, F., Murayama, T., Nickovic, S., Wilson, W.E., Sassen, K., Sugimoto, N., Malm, W.C., 2001. Asian dust events of April 1998. Journal of Geophysical Research 106, 18137–18330.

In, H.-J., Byun, D.W., Park, R.J., Moon, N.-K., Kim, S., Zhong, S., 2007. Impact of transboundary transport of carbonaceous aerosols on the regional air quality in the United States: a case study of the South American wildland fire of May 1998. Journal of Geophysical Research 112, D07201. doi:10.1029/2006JD007544.

Jaffe, D., Bertschi, I., Jaegle, L., Novelli, P., Reid, J.S., Tanimoto, H., Vingarzan, R., Westphal, D.L., 2004. Long-range transport of Siberian biomass burning emissions and impact on surface ozone in western North America. Geophysical Research Letters 31, L16106. doi:10.1029/2004GL020093.

Jo, W.K., Park, J.H., 2005. Characteristics of roadside air pollution in Korean metropolitan city (Daegu) over last 5 to 6 years: temporal variations, standard exceedances, and dependence on meteorological conditions. Chemosphere 59 (11), 1557–1573.

Jost, H.-J., Drdla, K., Stohl, A., Pfister, L., Loewenstein, M., Lopez, J.P., Hudson, P.K., Murphy, D.M., Cziczo, D.J., Fromm, M., Bui, T.P., Dean-Day, J., Gerbig, C., Mahoney, M.J., Richard, E.C., Spichtinger, N., Pittman, J.V., Weinstock, E.M., Wilson, J.C., Xueref, I., 2004. In-situ observations of mid-latitude forest fire plumes deep in the stratosphere. Geophysical Research Letters 31, L11101. doi:10.1029/2003GL019253.

Kaneyasu, N., Igarashi, Y., Sawa, Y., Takahashi, H., Takada, H., Kumata, H., Höller, R., 2007. Chemical and optical properties of 2003 Siberian forest fire smoke observed at the summit of Mt. Fuji, Japan. Journal of Geophysical Research 112, D13214. doi:10.1029/2007JD008544.

Kiehl, J.T., Hack, J.J., Bonan, G.B., Boville, B.A., Williamson, D.L., Rasch, P.J., 1998. The national center for atmospheric research community climate model: CCM3. Journal of Climate 11, 1131–1149.

King, M.D., Kaufman, J.Y., Tanré, D., Nakajima, T., 1999. Remote sensing of tropospheric aerosols from space: past, present, and future. Bulletin of American Meteorological Society 80, 2229–2259.

KME (Korea Ministry of Environment), 2007. Environmental Statistics Yearbook 2007, Seoul, p. 704 (in Korean).

Lapina, K., Honrath, R.E., Owen, R.C., Val Martin, M., Pfister, G., 2006. Evidence of significant large-scale impacts of boreal fires on ozone levels in the midlatitude Northern Hemisphere free troposphere. Geophysical Research Letters 33, L10815. doi:10.1029/2006GL025878.

Lavoué, D., Liousse, C., Cachier, H., Stocks, B.J., Goldammer, J.G., 2000. Modeling of carbonaceous particles emitted by boreal and temperate wildfires at northern latitudes. Journal of Geophysical Research 105, 26,871–26,890.

Lee, K.H., Kim, J.E., Kim, Y.J., Kim, J., Von Hoyningen-Huene, W., 2005. Impact of the smoke aerosol from Russian forest fires on the atmospheric environment over Korea during May 2003. Atmospheric Environment 39, 85–99.

Li, Z., Khananian, A., Fraser, R.H., Cihlar, J., 2001. Automatic detection of fire smoke using artificial neural networks and threshold approaches applied to AVHRR imagery. IEEE Transactions on Geoscience and Remote Sensing 39, 1859–1870.

Liu, Y., Park, R.J., Jacob, D.J., Li, Q., Kilaru, V., Sarnat, J.A., 2004. Mapping surface concentrations of fine particulate matter using MISR satellite observations of aerosol optical thickness. Journal of Geophysical Research 109, D22206. doi:10.1029/2004JD005025.

Liu, Y.Q., 2005. Enhancement of the 1988 northern U.S. drought due to wildfires. Geophysical Research Letters 32, L10806. doi:10.1029/2005GL022411.

Malevsky-Malevich, S.P., Molkentin, E.K., Nadyozhina, E.D., Shklyarevich, O.B., 2008. An assessment of potential change in wildfire activity in the Russian boreal forest zone induced by climate warming during the twenty-first century. Climate Change 86, 463–474. doi:10.1007/s10584-007-9295-7.

Martin, R.V., Jacob, D.J., Yantosca, R.M., Chin, M., Ginoux, P., 2003. Global and regional decreases in tropospheric oxidants from photochemical effects of aerosols. Journal of Geophysical Research 108 (D3), 4097. doi:10.1029/2002JD002622.

Matsui, T., Kreidenweis, S.M., Pielke Sr., R.A., Schichtel, B., Yu, H., Chin, M., Chu, D.A., Niyogi, D., 2004. Regional comparison and assimilation of GOCART and MODIS aerosol optical depth across the eastern U.S. Geophysical Research Letters 31, L21101. doi:10.1029/2004GL021017.

Mattis, I., Ansmann, A., Wandinger, U., Müller, D., 2003. Unexpectedly high aerosol load in the free troposphere over central Europe in spring/summer 2003. Geophysical Research Letters 30 (22), 2178. doi:10.1029/2003GL018442.

Mazzoni, D., Logan, J.A., Diner, D., Kahn, R., Tong, L., Li, Q., 2007. A data-mining approach to associating MISR smoke plume heights with MODIS fire measurements. Remote Sensing of the Environment 107, 138–148.

McKeen, S.A., Wotawa, G., Parrish, D.D., Holloway, J.S., Buhr, M.P., Hübler, G., Fehsenfeld, F.C., Meagher, J.F., 2002. Ozone production from Canadian wildfires during June and July of 1995. Journal of Geophysical Research 107 (D14), 4192. doi:10.1029/2001JD000697.

Monahan, E.C., Spiel, D.E., Davidson, K.L., 1986. A model of marine aerosol generation via whitecaps and wave disruption. In: Monahan, E.C., Mac Niocaill, G. (Eds.), Oceanic Whitecapse. D. Reidel, Norwell, Mass, pp. 167–174.

Murayama, T., Müller, D., Wada, K., Shimziu, A., Sekiguchi, M., Tsukamoto, T., 2004. Characterization of Asian dust and Siberian smoke with multiwavelength Raman lidar over Tokyo, Japan in spring 2003. Geophysical Research Letters 31, L23103. doi:10.1029/2004GL021105.

Nedelec, P., Thouret, V., Brioude, J., Sauvage, B., Cammas, J.-P., Stohl, A., 2005. Extreme CO concentrations in the upper troposphere over northeast Asia in June 2003 from the in situ MOZAIC aircraft data. Geophysical Research Letters 32, L14807. doi:10.1029/2005GL023141.

Park, R.J., Jacob, D.J., Chin, M., Martin, R.V., 2003. Sources of carbonaceous aerosols over the United States and implications for natural visibility. Journal of Geophysical Research 108 (D12), 4355. doi:10.1029/2002JD003190.

Park, R.J., Jacob, D.J., Field, B.D., Yantosca, R.M., Chin, M., 2004. Natural and transboundary pollution influences on sulfate-nitrate-ammonium aerosols in the United States: implications for policy. Journal of Geophysical Research 109, D15204.

Park, R.J., Jacob, D.J., Kumar, N., Yantosca, R.M., 2006. Regional visibility statistics in the United States: natural and transboundary pollution influences, and implications for the Regional Haze Rule. Atmospheric Environment 40 (28), 5405–5423.

Park, R.J., Jacob, D.J., Logan, J.A., 2007. Fire and biofuel contributions to annual mean aerosol mass concentrations in the United States. Atmospheric Environment 41, 7389–7400.

Park, R.J., Jacob, D.J., Palmer, P.I., Clarke, A.D., Weber, R.J., Zondlo, M.A., Eisele, F.L., Bandy, A.R., Thornton, D.C., Sachse, G.W., Bond, T.C., 2005. Export efficiency of black carbon aerosol in continental outflow: global implications. Journal of Geophysical Research 110, D11205. doi:10.1029/2004JD005432.

Park, S.U., In, H.J., 2003. Parameterization of dust emission for the simulation of the Yellow Sand (Asian dust) observed in March 2002 in Korea. Journal of Geophysical Research 108. doi:10.1029/2003JD003484.

Pfister, G.G., Hess, P.G., Emmons, L.K., Rasch, P.J., Vitt, F.M., 2008. Impact of the summer 2004 Alaska fires on top of the atmosphere clear-sky radiation fluxes. Journal of Geophysical Research 113, D02204. doi:10.1029/2007JD008797.

Real, E., Law, K.S., Weinzierl, B., Fiebig, M., Petzold, A., Wild, O., Methven, J., Arnold, S., Stohl, A., Huntrieser, H., Roiger, A., Schlager, H., Stewart, D., Avery, M., Sachse, G., Browell, E., Ferrare, R., Blake, D., 2007. Processes influencing ozone levels in Alaskan forest fire plumes during long-range transport over the North Atlantic. Journal of Geophysical Research 112, D10S41. doi:10.1029/2006JD007576.

Remer, L.A., Kaufman, Y.J., Tanré, D., Mattoo, S., Chu, D.A., Martins, J.V., Li, R.-R., Ichoku, C., Levy, R.C., Kleidman, R.G., Eck, T.F., Vermote, E., Holben, B.N., 2005. The MODIS aerosol algorithm, products, and validation. Journal of Atmospheric Sciences 62, 947–973.

Schaapa, M., Timmermansa, R.M.A., Koelemeijerb, R.B.A., de Leeuwa, G., Builtjesa, P.J.H., 2008. Evaluation of MODIS aerosol optical thickness over Europe using sun photometer observations. Atmospheric Environment. doi:10.1016/j.atmosenv.2007.11.044.

Soja, A.J., Tchebakova, N.M., French, N.H.F., Flannigan, M.D., Shugart, H.H., Stocks, B.J., Sukhinin, A.I., Parfenova, E.I., Chapin, F.S.I.I.I., Stackhouse Jr., P.W., 2007. Climate-induced boreal forest change: predictions versus current observations. Global and Planetary Change 56, 274–296.

Spracklen, D.V., Logan, J.A., Mickley, L.J., Park, R.J., Yevich, R., Westerling, A.L., Jaffe, D., 2007. Wildfires drive interannual variability of organic carbon aerosol in the western U.S. in summer. Geophysical Research Letters 34, L16816. doi:10.1029/2007GL030037.

Stocks, B.J., Fosberg, M.A., Lynham, T.J., Mearns, L., Wotton, B.M., Yang, Q., Jin, J.-Z., Lawrence, K., Hartley, G.R., Mason, J.A., McKenney, D.W., 1998. Climate change and forest fire potential in Russian and Canadian boreal forests. Climate Change 38 (1), 1–13.

Turpin, B.J., Lim, H.J., 2001. Species contributions to PM$_{2.5}$ mass concentrations: revisiting common assumptions for estimating organic mass. Aerosol Science and Technology 35, 602–610.

Turquety, S., Logan, J.A., Jacob, D.J., Hudman, R.C., Leung, F.Y., Heald, C.L., Yantosca, R.M., Wu, S., Emmons, L.K., Edwards, D.P., Sachse, G.W., 2007. Inventory of boreal fire emissions for North America in 2004: importance of peat burning and pyroconvective injection. Journal of Geophysical Research 112, D12S03. doi:10.1029/2006JD007281.

van der Werf, G.R., Randerson, J.T., Giglio, L., Collatz, G.J., Kasibhatla, P.S., Arellano, A.F., 2006. Interannual variability in global biomass burning emissions from 1997 to 2004. Atmospheric Chemistry and Physics 6, 3423–3441.

Westerling, A.L., Hidalgo, H.G., Cayan, D.R., Swetnam, T.W., 2006. Warming and earlier spring increase western US forest wildfire activity. Science 313 (5789), 940–943.

Wiscombe, W., 1980. Improved Mie scattering algorithms. Applied Optics 19, 1505–1509.

Wotawa, G., Novelli, P.C., Trainer, M., Granier, C., 2001. Inter-annual variability of summertime CO concentrations in the Northern Hemisphere explained by boreal forest fires in North America and Russia. Geophysical Research Letters 28, 4575–4578.

Wotawa, G., Trainer, M., 2000. The influence of Canadian forest fires on pollutant concentrations in the United States. Science 288, 324–328.

Yihui, D., Chan, J.C.L., 2005. The East Asian summer monsoon: an overview. Meteorology and Atmospheric Physics 89 (1–4), 117–142. doi:10.1007/s00703-005-0125-z.

Zhang, Y., Arimoto, R., An, Z., Chen, T., Zhang, G., Zhu, G., Wang, X., 1993. Atmospheric trace elements over source regions for chinese dust: concentrations, sources and atmospheric deposition on the loess plateau. Atmospheric Environment 27, 2051–2067.

Zender, C.S., Bian, H., Newman, D., 2003a. Mineral Dust Entrainment and Deposition (DEAD) model: description and 1990s dust climatology. Journal of Geophysical Research 108 (D14), 4416. doi:10.1029/2002JD002775.

Zender, C.S., Newman, D., Torres, O., 2003b. Spatial heterogeneity in aeolian erodibility: uniform, topographic, geomorphic, and hydrologic hypotheses. Journal of Geophysical Research 108 (D17), 4543. doi:10.1029/2002JD003039.